Journal of Physiology (1989), **415**, *pp.* 503–531
With 11 *text-figures*
Printed in Great Britain

SINGLE SODIUM CHANNELS FROM CANINE VENTRICULAR MYOCYTES: VOLTAGE DEPENDENCE AND RELATIVE RATES OF ACTIVATION AND INACTIVATION

BY M. F. BERMAN*, J. S. CAMARDO†, R. B. ROBINSON AND S. A. SIEGELBAUM

From the Departments of Pharmacology, Anesthesiology, and the Howard Hughes Medical Institute, Columbia University, College of Physicians and Surgeons, 630 W. 168 Street, New York, NY 10032, USA*

(*Received 2 November 1988*)

SUMMARY

1. Single sodium channel currents were recorded from canine ventricular myocytes in cell-attached patches. The relative rates of single-channel activation *vs.* inactivation as well as the voltage dependence of the rate of open-channel inactivation were studied.

2. Ensemble-averaged sodium currents showed relatively normal activation and inactivation kinetics, although the mid-point of the steady-state inactivation (h_∞) curve was shifted by 20–30 mV in the hyperpolarizing direction. This shift was due to the bath solution, which contained isotonic KCl to depolarize the cell to 0 mV.

3. Steady-state activation showed less of a voltage shift. The threshold for eliciting channel opening was around −70 mV and the mid-point of activation occurred near −50 mV.

4. The decline of the ensemble-averaged sodium current during a maintained depolarization was fitted by a single exponential function characterizing the apparent time constant of inactivation (τ_h). The apparent rate of inactivation was voltage dependent, with τ_h decreasing e-fold for a 15·4 mV depolarization.

5. The relative contributions of the rates of single-channel activation and inactivation in determining the time course of current decay (τ_h) were examined using the approach of Aldrich, Corey & Stevens (1983). Mean channel open time (τ_o) showed significant voltage dependence, increasing from 0·5 ms at −70 mV to around 0·8 ms at −40 mV. At −70 mV τ_h was much greater than τ_o, while at −40 mV the two time constants were similar.

6. The degree to which the kinetics of single-channel activation contribute to τ_h was studied using the first latency distribution. The first latency function was fitted by two exponentials. The slow component was voltage dependent, decreasing from 19 ms at −70 mV to 0·5 ms at −40 mV. The fast component (0·1–0·5 ms) was not well resolved.

* To whom correspondence should be addressed.

† Present address: Department of Pharmacology, University of Pennsylvania, Philadelphia, PA 19104, USA.

7. Comparing the first latency distribution with the time course of the ensemble-averaged sodium current at −40 mV showed that activation is nearly complete by the time of peak inward sodium current. However, at −70 mV, activation overlaps significantly with the apparent time course of inactivation of the ensemble-averaged current.

8. Using the methods of Aldrich *et al.* (1983) we also measured the apparent rate of open-channel closing (*a*) and open-channel inactivation (*b*). Both rates were voltage dependent, with *a* showing an e-fold decrease for an 11 mV depolarization and *b* showing an e-fold increase for a 30 mV depolarization.

9. We conclude that at relatively depolarized potentials, the apparent time course of inactivation of the macroscopic sodium current (τ_h) is largely determined by the microscopic rate of open-channel inactivation. At more negative potentials, near threshold for sodium channel activation, both inactivation and activation processes contribute to determining τ_h. The rate of open-channel inactivation is voltage dependent, although the extent of voltage dependence is roughly one-third that of the activation process.

INTRODUCTION

In response to a step voltage-clamp depolarization, the cardiac sodium current rises rapidly to a peak inward value and then more slowly decays from that peak (see Fozzard, January & Makielski, 1985 for review). Most voltage-clamp studies have used a Hodgkin–Huxley analysis (Hodgkin & Huxley, 1952) to characterize channel kinetics in terms of an activation reaction that controls the rising phase of the sodium current and an inactivation reaction that controls the declining phase. This approach assumes independent activation (m) and inactivation (h) gating reactions and that the rate of channel activation is much faster than the rate of inactivation. Accordingly, the microscopic rates of channel activation and inactivation can be obtained by fitting exponential functions to the rising and falling phases of the macroscopic sodium current, respectively.

Although there is good evidence that sodium channel activation is indeed rapid compared to inactivation in the squid giant axon (Bezanilla & Armstrong, 1977) and in frog skeletal muscle (Gonoi & Hille, 1987), Aldrich *et al.* (1983) have used single-channel recording to show that in neuroblastoma activation can be quite slow compared to inactivation. Because of the resulting overlap in the time course of single-channel activation and inactivation, the time course of decay of the neuroblastoma sodium current is determined largely by the slow rate of activation. As a result, measurements of the time constant of macroscopic current decay do not provide an accurate measure of the true microscopic rate of channel inactivation. For example, Aldrich *et al.* (1983), in agreement with others, have found that the apparent voltage dependence of sodium current inactivation is not due to a true voltage-dependent inactivation of open sodium channels but rather is a reflection of the voltage dependence of channel activation.

Do cardiac sodium channels behave like neuroblastoma sodium channels or are they more like squid axon sodium channels? The question is of importance for understanding the kinetic basis for cardiac sodium channel function and for interpreting results of pharmacological experiments that have used measurements

of τ_h to infer mechanisms for anti-arrhythmic drug action. Despite an increasing number of studies of single cardiac sodium channel properties (Cachelin, De Peyer, Kokubun & Reuter, 1983; Grant, Starmer & Strauss, 1983; Kunze, Lacerda, Wilson & Brown, 1985; Patlak & Ortiz, 1985; Grant & Starmer, 1987), the question of the relative rates of cardiac sodium channel activation and inactivation has not been directly addressed. In this paper we have used the general approach of Aldrich *et al.* (1983) to determine the kinetics of cardiac sodium channel activation and inactivation. In addition, we have used this approach to estimate the microscopic rates of open-channel inactivation at different membrane potentials. Our results show that at relatively depolarized potentials, the apparent time course of inactivation of the macroscopic sodium current (τ_h) is largely determined by the microscopic rate of open-channel inactivation. At more negative potentials, near threshold for sodium channel activation, both inactivation and activation processes contribute to τ_h. Finally, the rate of open-channel inactivation is inherently voltage dependent, although the extent of the voltage dependence is roughly one-third that of the activation process. Some of these results have appeared in an abstract (Siegelbaum, Camardo & Robinson, 1986).

METHODS

Preparation and solutions

Cardiac myocytes were obtained from adult canine ventricle according to the method of Hewett, Legato, Danilo & Robinson, (1983). Dogs of either sex were anaesthetized with pentobarbitone sodium (30 mg kg^{-1} I.V.), their hearts removed quickly and a wedge of left ventricular free wall obtained for collagenase digestion. Normally, the cells were stored in Krebs solution in 95% O_2–5% CO_2 at 37 °C and used within 8 h. In one experiment (the single-channel patch, see below), cells were stored overnight at 4 °C and used the next day.

Patch pipettes were fabricated from Boralex capillary tubes (Dynalab, Rochester, NY, USA) using a standard two-stage pull with a List pipette puller. The pipettes were coated with a double layer of Sylgard (Dow Corning 184) to within 100 μm of the tip and fire-polished. When filled with normal Tyrode solution (see below), pipettes had resistances of 5–10 MΩ.

Experiments were performed with the cells depolarized to 0 mV in a high potassium solution containing (in mM): 150 KCl, 2 $MgCl_2$, 10 HEPES and 10 glucose at pH 7·2. The pipette was filled with normal Tyrode solution, containing (in mM): 145 NaCl, 4 KCl, 1·8 $CaCl_2$, 2 $MgCl_2$ and 10 HEPES at pH 7·2. In the experiment with a single channel in the patch the bath contained a zero calcium solution (in mM): 120 potassium glutamate, 25 KCl, 1 $MgCl_2$, 1 EGTA and 10 HEPES at pH 7·2. Experiments were performed at 19–21 °C.

Experimental protocol

Single-channel currents were recorded from cell-attached patches using a List EPC-7 patch-clamp amplifier (Hamill, Marty, Neher, Sakmann & Sigworth, 1981). The output of the amplifier was filtered at 2·0 kHz (3 dB down) with an 8-pole Bessel filter (Frequency Devices). Command voltage clamp pulses were applied using a DEC LSI 11/73 computer with an INDEC Systems (Sunnyvale, CA, USA) laboratory interface. Data were sampled using a 12 bit A/D converter at 10 kHz and stored on hard disc for later analysis.

Forty millisecond long step-depolarizations were applied to the cell attached patches from negative holding potentials (V_h) to test potentials (V_t) between −70 and −40 mV at a rate of 1–2 Hz. The holding potential for each test potential was selected to inactivate a significant fraction of channels in the patch to minimize the number of overlapping openings and to obtain an adequate number of sweeps with no openings (null sweeps) to perform an Aldrich, Corey and Stevens analysis. In general, holding potentials were chosen so that channel openings were observed in about half of all sweeps, corresponding to a holding potential of −120 to −95 mV.

Steady-state inactivation curves were obtained by holding the patch at a series of different

potentials from −140 to −90 mV and stepping to a constant test potential (generally −40 mV). Peak normalized ensemble-averaged currents were measured and fitted by a standard Hodgkin–Huxley inactivation curve of the form:

$$h_\infty = \frac{1}{1-\exp[(V-V')/k]} \tag{1}$$

using a non-linear least-squares fitting routine.

Single-channel analysis

Linear leak and capacitative currents were subtracted from all records. Idealized records were created using a channel detection routine and a threshold equal to half the channel amplitude. A linear interpolation was used between data points just above and below the threshold to define the transition time at a nominal resolution of 2 × sampling frequency. In some cases we compared these results with those obtained using a cubic spline routine to interpolate eight points between each pair of samples. After the first 200 μs in the lifetime histograms, no significant difference was detected between these two methods. In cases where there were overlapping openings, a particular closing was assigned to a particular opening using a random number generator. Such overlapping events accounted for less than 5% of openings in a typical experiment.

Histograms of channel open times, closed times and first latencies to opening were constructed. Open-time histograms were fitted by a single exponential function using the method of maximum likelihood and a simplex algorithm, including a correction for missed events briefer than our 200 μsec threshold. Cumulative first latency distributions $P_1(t)$ (i.e. the probability that the first opening in a sweep occurs after time t) were fitted by the sum of two exponential functions (see Theory).

THEORY

First latency distribution

Following previous studies of single sodium channel activation (Aldrich *et al.* 1983; Horn & Vandenberg, 1984; Kunze *et al.* 1985), we assume that channel activation can be described by the following general model:

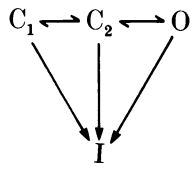

This model predicts that the first latency distribution for a single channel is described by the sum of two exponential functions of following form (Aldrich *et al.* 1983):

$$P_1(t) = [1-P(0)][\tau_{12}\exp(-t/\tau_{11}) - \tau_{11}\exp(-t/\tau_{12})]/(\tau_{12}-\tau_{11}), \tag{2}$$

where τ_{11} and τ_{12} are the two exponential time constants and $P(0)$ is the probability that a resting channel never opens (i.e. the probability that it directly enters the inactivated state).

In practice, the observed first latency distribution also depends on the number of channels in the patch and the extent of resting inactivation (h_∞). The first latency function for an N channel patch, $P_1^N(t)$, is a power series of eqn (2) that depends on the number of available (resting) channels, k, at the start of each depolarizing sweep:

$$P_1^N(t) = \sum_{k=1}^{N} P_r(k)\,P_1(t)^k,$$

where $P_r(k)$ is the probability that k out of N channels are in the resting state (non-inactivated) at the start of a sweep. This probability $P_r(k)$ depends on N and h_∞ according to the binomial distribution, thus:

$$P_1^N(t) = \sum_{k=1}^{N} \frac{N!}{(N-k)!\,k!} (h_\infty)^k (1-h_\infty)^{(N-k)} P_1(t)^k. \tag{3}$$

An estimate for N was obtained by counting the maximal number of overlapping events using a negative holding potential (−140 mV) where h_∞ is maximal and stepping to a relatively positive test potential (−40 mV) where channels rapidly activate. Most patches had multiple channels, with N ranging from three to ten. One patch contained only a single active channel.

Markov analysis of transition probabilities and rates

One goal of these studies was to measure the transition probabilities for channel opening and inactivation as well as the rates for these processes. According to the general model shown above, sodium channels exist in a closed resting state (C_1 or C_2), a non-conducting inactive state (I), or an open state (O). Upon depolarization, channels either enter the inactive state or pass transiently into the open state. Once a channel opens, it closes back to the resting state or inactivates. Because the inactive state is absorbing, once a channel inactivates, it remains inactivated until the membrane is repolarized.

The approach of Kunze *et al.* (1985) involves determining two probabilities: A, the transition probability that a resting channel opens; and R, the probability that an open channel reopens, rather than inactivates. The value for A can be determined from the percentage of sweeps with no openings (null sweeps). For a single-channel patch with no resting inactivation, the probability of observing a null sweep is given by $(1-A)$. For an N channel patch where $h_\infty < 1$,

$$P(0) = (1-h_\infty A)^N. \tag{4}$$

The parameter R is obtained by using the relationship that, for a single-channel patch with no resting inactivation, the mean number of openings per sweep ($\bar{j}$) is given by $A/(1-R)$. For a patch with N channels and some degree of resting inactivation, the following equation applies:

$$\bar{j} = \frac{Nh_\infty A}{1-R}. \tag{5}$$

Although the transition probabilities A and R can be obtained in this manner, the general two-closed-state model has too many free parameters to allow us to solve exactly for other probabilities or the rates of any of the transitions. In cases where inactivation only occurs from state C_2, the general model reduces to the following simplified model of Aldrich *et al.* (1983), which provides an approximate description of sodium channel kinetics that can be solved more completely:

(M1)

Here, A is still the transition probability that a resting channel opens, and B is the probability that an open channel closes back to the resting state. In this definition a is the rate at which an open channel closes and b is the rate at which an open channel inactivates.

From the model (M1), the mean channel open time τ_o is given by

$$\tau_o = 1/(a+b), \tag{6}$$

and the probability that an open channel closes to the resting state is given by:

$$B = a/(a+b). \tag{7}$$

Aldrich *et al.* showed that the mean number of openings per sweep, $\bar{j}$, for a single-channel patch with no resting inactivation is given by $A/(1-AB)$. For a patch containing N channels with some resting inactivation, the following equation applies:

$$\bar{j} = \frac{Nh_\infty A}{1-AB}. \tag{8}$$

The probability A can be derived from the number of null sweeps as shown earlier in eqn (4), and B is then derived from eqn (8). Finally, from B and τ_o we can determine the rates a and b.

Recently, the applicability of the simple model (M1) has been questioned since the method of Aldrich *et al.* can yield probabilities greater than one or negative rate constants in certain preparations (Vandenberg & Horn, 1984; Kunze *et al.* 1985). We have therefore taken the approach of first determining the model-independent probabilities A and R from our data and then deriving the model-dependent probability B and rates a and b. In practice, the true values for τ_o, $P(0)$ and $\bar{j}$ differ from the observed experimental values τ_o', $P(0)'$ and $\bar{j}'$ due to the bandwidth limitations of data acquisition. A correction procedure (see Appendix) was applied to the data to compensate for these errors.

Sources of error

With the above analyses it is necessary to measure: (1) the mean channel open time (τ_o); (2) the probability of observing a sweep with no openings, $P(0)$; and (3) the mean number of openings per sweep ($\bar{j}$). There are three possible sources of error in these measurements due to the limited bandwidth of our recordings and baseline noise. The first comes from an overestimate of the mean open time due to missed brief closings within an opening (Colquhoun & Sigworth, 1983). At depolarized test potentials, channel reopening is rare (due to the very slow closing rate and fast inactivation rate) and this problem is negligible. Also at very negative test potentials, where reopening is more common, the mean closed time is relatively long due to the slow rate of activation. In this situation few closings will be missed. At intermediate test potentials (-60 or -50 mV), missed closings could introduce errors. We applied a correction for missed events to the apparent mean open time (τ_o) using a procedure modified from Colquhoun & Sigworth (1983) appropriate for the kinetic scheme of model (M1) (see Appendix). In practice this correction changed the mean open and closed times by less than 10%.

A second error results from an underestimate of the mean number of openings per sweep ($\bar{j}$) due to missed closings and missed openings. Using a 50% amplitude detection threshold, all openings and closings shorter than $Q = 0{\cdot}179/f_c$ s, where Q is the minimum duration for an event to be detected and f_c is the low-pass cut-off frequency, will be missed (Colquhoun & Sigworth, 1983). A correction was applied to account for missed openings given by $\bar{j} = \bar{j}' \exp(Q/\tau_o)$, where $\bar{j}'$ is the observed mean number of openings per sweep and τ_o is the mean open time (Colquhoun & Sigworth, 1983; Kunze *et al.* 1985). Missed openings will also result in an overestimate of the probability of a null sweep, $P(0)$. The observed $P(0)'$ was corrected for missed openings according to the method of Kunze *et al.* (1985).

The third potential source of error in detecting events comes from false openings due to random baseline noise that exceeds the channel detection threshold. Two methods were used to estimate the extent of this problem. First, we applied the theoretical treatment of Colquhoun & Sigworth (1983) based on measured baseline noise and the predicted Gaussian distribution of current amplitude. The r.m.s. noise from 50 Hz to 2 kHz using stretches of data with no channel openings was $< 0{\cdot}15$ pA and the ratio of detection threshold to r.m.s. noise averaged $4{\cdot}9 \pm 0{\cdot}5$ for all patches. The highest false event rate computed from this range is 0·2 per second, which corresponds to a probability equal to 0·008 of observing at least one false event in a 40 ms sweep. The second method for estimating false events was empirical and involved measuring false openings from stretches of data where no true channel openings are expected (e.g. using a depolarized holding potential). With this method, we detected false events at a rate of 0–0·5 per hundred sweeps. Accordingly, no correction for false events was employed.

To minimize variability resulting from differences between patches, we organized our data collection in a manner that would allow us to record sodium channel kinetics at several different test potentials using the same patch. Test potentials from -70 to -40 mV were selected because negative to -70 mV there were too few channel openings and positive to -40 mV the single-channel amplitude was too small.

In multichannel patches, it was often difficult to measure accurately the probability that no channels open during a sweep, $P(0)$, since there were very few null sweeps. To increase the fraction of sweeps with no openings we generally used a depolarized holding potential where h_∞ was small. To then extract the probability that a resting channel opens, rather than inactivates, it is necessary to determine the value of h_∞ (see eqn (4)). To ensure accuracy in measuring h_∞, resting inactivation curves were recorded several times during an experiment, often bracketing a single test run with separate inactivation curves.

One possible problem in these experiments is that the relatively depolarized holding potentials (relative to potentials where $h_\infty = 1$) after the normal kinetics of activation (cf. Grant & Starmer, 1987), possibly by shifting resting channels into a closed state that lies closer to the channel open state (e.g. Armstrong & Bezanilla, 1977). To test for possible influences of holding potential on channel kinetics, we compared ensemble-averaged sodium currents obtained from a holding potential of -140 mV, where $h_\infty = 1$, with currents from a more depolarized holding potential (e.g. -100 to -110 mV) where $h_\infty < 1$. As shown in Fig. 1, there is little difference in the time course of the ensemble-averaged sodium current obtained from the two

holding potentials. In a minority of patches, we found that the kinetics of inactivation were 10–20% slower at the more depolarized holding potentials. This small effect of holding potential should not alter any of our qualitative conclusions.

In one experiment, with a patch that contained only a single sodium channel, it was possible to perform the entire channel protocol from a hyperpolarized holding potential where $h_\infty = 1$ ($V_h \leqslant -140$ mV). Results from this patch are consistent with results from multichannel patches held at less negative voltages.

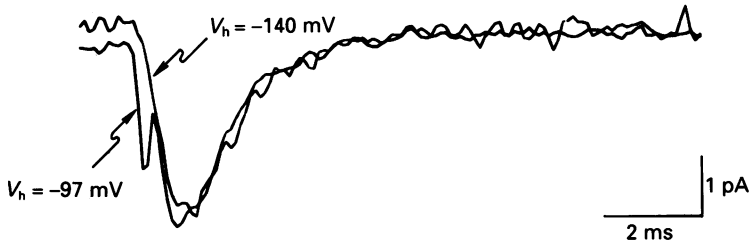

Fig. 1. Effect of holding potential on ensemble-averaged sodium currents. Superimposed records of sodium currents averaged from 300 to 400 individual sweeps from a holding potential of −97 mV or −140 mV, stepped to a test potential of −40 mV. Current amplitude arbitrarily scaled for comparison.

Two other potential sources of variability come from the possible presence of a second class of smaller amplitude sodium channels (Cachelin *et al.* 1983; Kunze *et al.* 1985) as well as unusually long bursts of channel openings that occur throughout the depolarizing pulse (Patlak & Ortiz, 1985). We find, using cell-attached patch recordings from canine ventricular myocytes a very low incidence (< 1%) of small conductance channels or of prolonged channel openings. Patches that showed small amplitude channels or prolonged bursts were not used in this analysis.

RESULTS

The first part of the Results section concentrates on records from a single patch containing six channels. The original histograms, fitted equations and derived parameters are shown for all four test potentials. Where appropriate we have included summary figures covering all eight multichannel patches. Calculation of the model-dependent rate and probability constants concludes the Results section. We have included a table of the more important measured and calculated parameters for all patches at all test potentials (Table 1).

Figure 2 shows representative single sodium channel current records from a cell-attached patch containing six active channels in response to depolarizing voltage steps to four different test potentials (indicated on the traces). Each group of records represents seven consecutive sweeps. The records show that with steps to −70 or −60 mV there are several channel openings per sweep. While this suggests that a single channel can open and close several times before inactivating, the multiple openings could reflect openings of independent channels since this patch contained six channels. The question of whether a single channel opens more than once during

a depolarization will be considered in more detail later. With the steps to −60 and −70 mV, channel openings occur throughout the depolarization and the first opening often occurs well after the start of the depolarization. With steps to more depolarized test potentials (e.g. −50 or −40 mV), there are fewer openings per sweep and the openings that do occur appear clustered near the beginning of the depolarization.

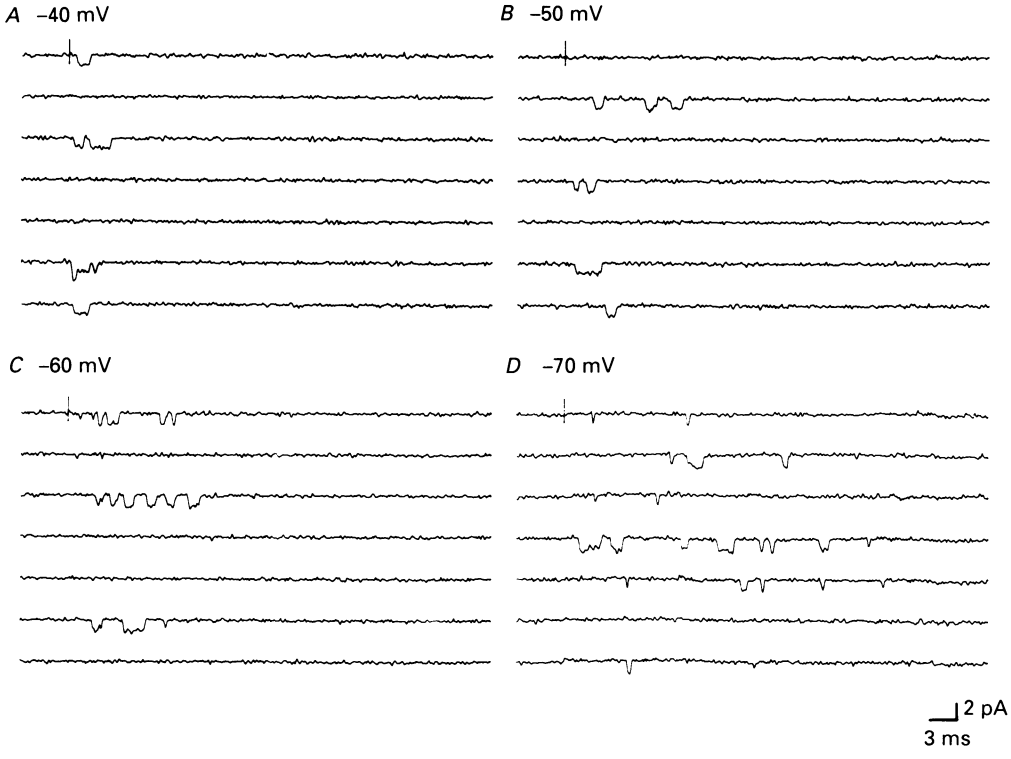

Fig. 2. Single sodium channel records at four test potentials. *A*, seven consecutive channel records in response to 40 ms long test depolarization to −40 mV from a holding potential of −97 mV. Vertical line indicates start of depolarizing pulses. *B*, records in response to steps to −50 mV, $V_h = -95$ mV. *C*, test depolarizations to −60 mV, $V_h = -95$ mV. *D*, test depolarizations to −70 mV, $V_h = -103$ mV. Current records filtered at 2 kHz.

Figure 3 shows the ensemble-averaged currents obtained in response to the four different depolarizations shown in Fig. 2. About 400 records were summed to obtain each average current, including sweeps with no apparent openings. A single exponential function has been fitted to the current decline to provide a measure of the apparent time constant of inactivation (τ_h) of the ensemble-averaged current. Openings in response to depolarizations to −70 mV, which is near the threshold for sodium channel activation, are so broadly distributed throughout the sweep that the ensemble-averaged current is small and noisy and does not yield a well resolved averaged current in this experiment. With larger depolarizations, more channels are activated and the time course of the averaged current gets faster, with an apparent increase in both the rate of activation and inactivation.

The relationship between steady-state inactivation, peak activation and membrane potential is plotted in Fig. 4*A*. Steady-state inactivation (h_∞) was measured by holding the patch at different potentials and then stepping the membrane to a constant test potential (−40 mV). For each potential the peak of the inward ensemble-averaged current was normalized by the largest peak current. These

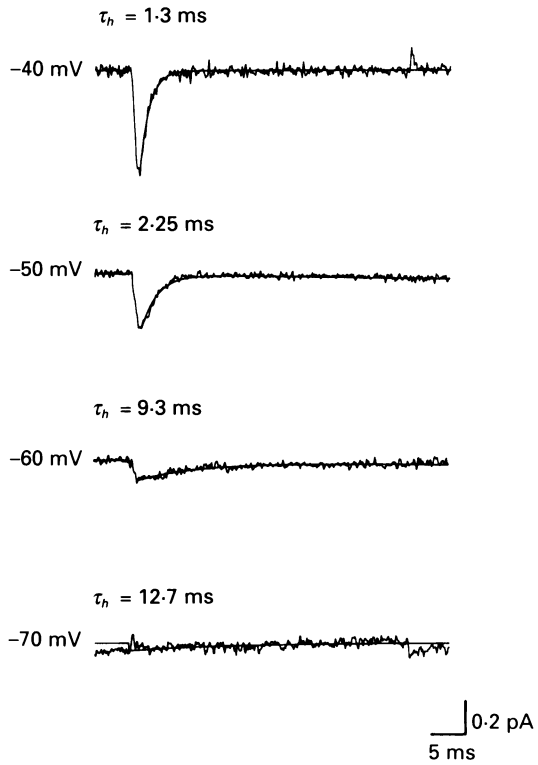

Fig. 3. Ensemble-averaged sodium currents at four different test potentials. Traces obtained from same experiment as shown in Fig. 2. Test voltages and holding potentials are also the same. Declining phase of inward current has been fitted by a single exponential function (smooth curve) to determine τ_h, apparent time constant of inactivation of ensemble-averaged current.

normalized peak currents are plotted as a function of holding potential in Fig. 4*A* (circles). The superimposed curve shows the best fitted Hodgkin–Huxley inactivation curve. In this patch the mid-point of inactivation (V') occurred at −103 mV and the slope of the curve (k) was 5·3 mV. For all patches, the mean value for V' was $-110{\cdot}6 \pm 4{\cdot}4$ mV ($\pm$S.D.) and the mean value for k was $4{\cdot}8 \pm 0{\cdot}8$ mV.

Figure 4*A* also demonstrates the relationship between test potential and the probability that a channel is open at the peak of the inward current, P_o(peak), shown as triangles. This was obtained from measurements of the peak ensemble-averaged inward current, I_p, where $I_p = NiP_o(\text{peak})h_\infty$. N is the number of channels in the patch and i is single-channel current amplitude.

Figure 4*B* plots the apparent time constant of inactivation (τ_h) for the decay phase of the ensemble-averaged currents for different test potentials. The data

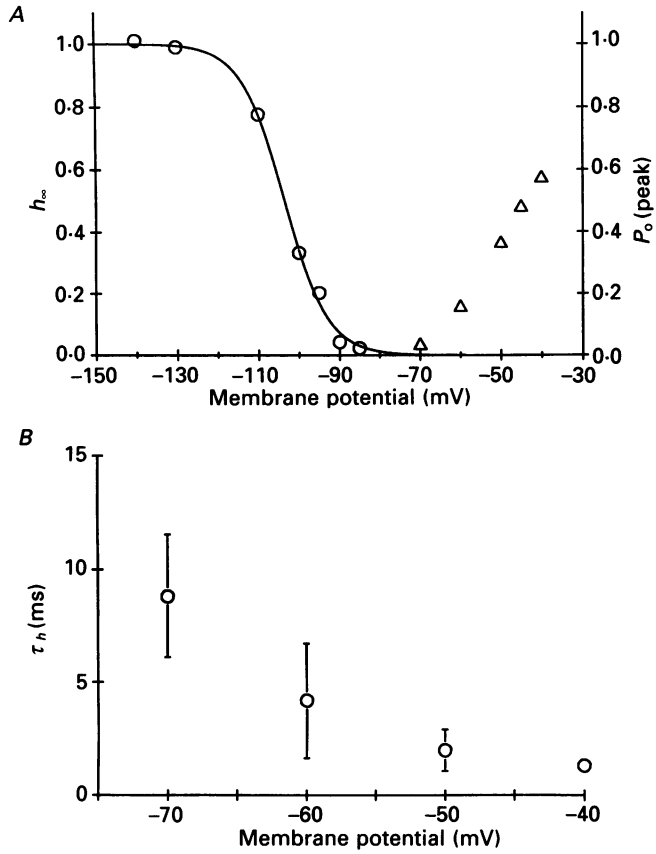

Fig. 4. *A*, voltage dependence of steady-state inactivation (h_∞) and peak activation P_o(peak). Inactivation measured from peak ensemble-averaged sodium currents in response to step to −40 mV test potential from different holding potentials. Peak currents normalized by maximal peak inward sodium current. Data fitted by standard Hodgkin–Huxley inactivation curve with $V' = -103$ mV and slope of 5·3 mV. Peak activation measured from ensemble-averaged peak sodium currents at different test potentials. Peak currents were normalized by product $Nh_\infty i$, where N is number of channels in a patch (6), h_∞ is measured steady-state inactivation and i is single-channel current amplitude at each test potential. Data from experiment shown in Fig. 2. *B*, relation of τ_h and membrane potential. Data points are averages from three to eight experiments. Error bars in this and all subsequent figures show standard deviation.

represent average values for τ_h obtained from all of our experiments. There is a clear voltage-dependent increase in the rate of inactivation as the membrane is depolarized, although there is some scatter when values are compared for different patches. The dependence of τ_h on membrane potential is also seen in the data for each individual patch (Table 1). The relationship between τ_h and test potential is approximately exponential, with τ_h decreasing e-fold for every 15·5 mV depolarization.

At the level of single-channel function, which kinetic process determines the rate of this apparently voltage-dependent inactivation of the ensemble-averaged current? The simplest possibility is that the time course of the ensemble-averaged current

inactivation reflects the distribution of single-channel open times. Figure 5 shows open time distributions at the four different test potentials. Single exponentials were fitted to the data using a maximum likelihood routine. At −70 mV, the open time distribution is quite brief, with a mean open time of around 0·4 ms. With stronger depolarizations the mean open time gets longer, reaching a maximum of 1·0 ms at −40 mV. Figure 6*A* shows the relationship between average mean open time and test potential obtained from all experiments. There is a clear trend for open time to increase at more positive test potentials. A detailed comparison of τ_0 and τ_h is presented in Fig. 6*B*, which shows data averaged from all the multichannel patch

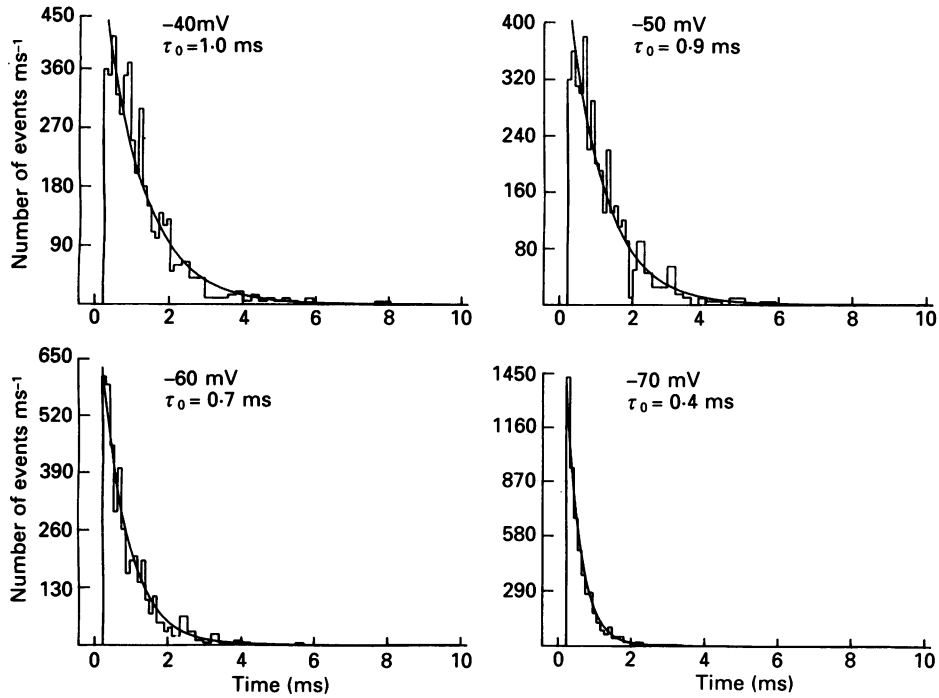

Fig. 5. Channel open time histograms at four different test potentials (indicated on each graph). Smooth curve is single exponential function fitted to data by maximum likelihood, yielding estimates for channel open time τ_0 (indicated on graphs). Experimental conditions as in Fig. 2.

experiments. There is a marked discrepancy between τ_0 and τ_h, especially at negative test potentials. However, at more positive test potentials the two time constants begin to converge, although τ_h is still longer than τ_0, even at −40 mV.

One possible explanation for the discrepancy between channel open time and the apparent time constant of inactivation from the ensemble-averaged currents is that kinetics of activation may, in part, determine the apparent time course of sodium current decay (Aldrich *et al.* 1983). To examine the time course of activation directly, we measured the first latency distribution for channel opening during depolarizing steps to test potentials from −70 to −40 mV. Cumulative first latency histograms obtained at four different test potentials in a single patch are shown in Fig. 7*A*. These histograms plot the observed probability, $P_1^N(t)$, that a channel first opens in a sweep

TABLE 1. Measured and calculated parameters

Experimental conditions			Parameters				Time constants			Calculated parameters		
ID No.	V_t (mV)	V_h (mV)	N	h_∞	$P(0)$	$\bar{j}'$	τ_o (ms)	τ_h (ms)	τ_{11} (ms)	$\bar{j}_b$	a (ms^{-1})	b (ms^{-1})
A09A	−40	−100	8	0·14	0·38	1·02	0·77	1·10	0·39	1·13	160	1139
	−50	−105	8	0·16	0·33	1·23	0·87	1·86	0·88	1·27	280	865
	−60	−110	8	0·27	0·21	2·32	0·67	2·72	1·18	1·72	866	632
	−70	−110	8	0·23	0·24	2·90	0·55	6·20	4·52	2·46	1397	413
H04A	−40	−90	10	0·05	0·62	0·52	0·72	1·49	0·69	1·15	169	1224
	−50	−95	10	0·11	0·50	1·04	0·71	4·00	0·82	1·63	792	611
	−60	−90	10	0·05	0·83	0·30	0·49	6·01	7·19	1·70	1925	120
H08B	−40	−97	6	0·22	0·24	1·36	1·02	1·33	0·48	1·09	80	904
	−50	−95	6	0·12	0·47	1·12	0·91	2·35	0·86	1·63	388	715
	−60	−95	6	0·18	0·56	1·22	0·67	7·46	3·67	2·43	—	—
	−70	−103	6	0·32	0·34	1·61	0·38	13·07	18·90	1·80	2011	647
H47A	−50	−120	4	0·74	0·01	3·44	0·80	1·41	0·46	1·31	298	951
	−60	−110	4	0·44	0·21	2·17	0·66	3·37	1·73	1·80	860	654
H71A	−50	−95	6	0·06	0·73	0·42	0·65	1·45	0·70	1·46	514	1017
	−70	−95	6	0·06	0·86	0·28	0·44	9·70	14·40	2·10	—	—
H72B	−50	−150	4	1·00	0·03	2·88	0·63	2·06	1·09	1·29	548	1034
	−70	−150	4	1·00	0·07	3·41	0·44	7·22	4·02	1·95	2085	214
H77A	−50	−110	3	0·234	0·45	0·78	0·89	1·48	0·37	1·14	123	1004
	−70	−110	3	0·234	0·71	0·74	0·56	—	3·99	2·53	—	—
H77B	−50	−105	4	0·18	0·57	0·57	0·59	1·17	0·32	1·11	215	1486
	−60	−110	4	0·37	0·44	0·96	0·65	1·25	0·98	1·35	728	801
	−70	−110	4	0·37	0·46	1·38	0·50	7·83	4·11	2·15	—	—
A19E	−30	−150	1	1·00	0·25	0·85	0·50	0·76	0·31	1·16	324	1680
	−40	−140	1	1·00	0·24	1·17	0·85	2·56	1·28	1·60	544	635
	−50	−140	1	1·00	0·25	1·42	0·66	3·62	1·37	2·03	952	552
	−60	−140	1	1·00	0·39	1·62	0·55	12·05	10·47	2·07	1425	393
	−70	−140	1	1·00	0·77	0·29	0·31	—	67·53	1·33	2798	418

after a given time t. The non-zero steady-state probability of these distributions reflects the probability of observing a sweep with no openings. Based on the general two closed-state model for activation, each first latency distribution was fitted by a function consisting of the sum of two exponentials (see eqn (3)). The time constant of the slow (major) exponential, τ_{l1}, shows a clear dependence on membrane

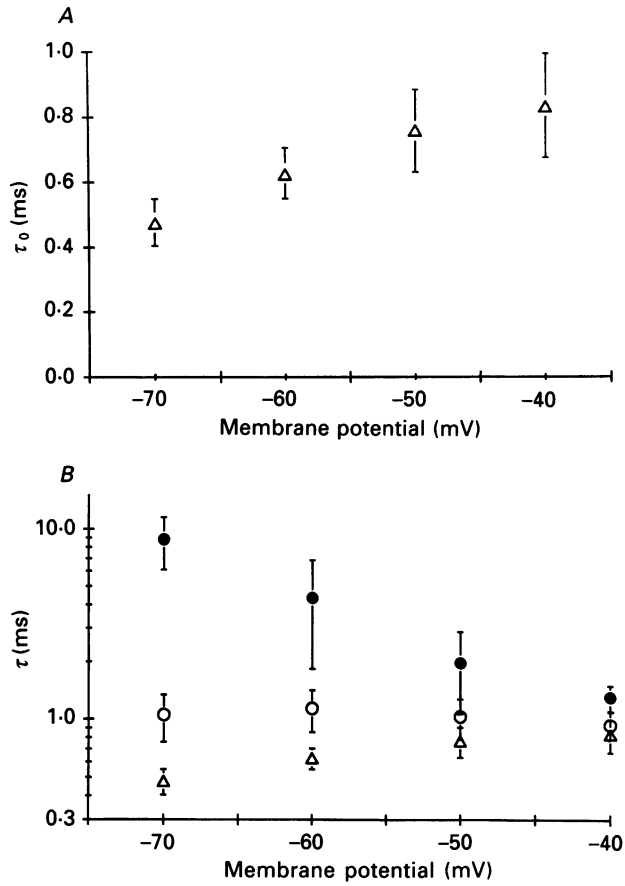

Fig. 6. *A*, relation between channel open time and test potential. Data averaged from three to eight experiments. *B*, comparison of channel open time (τ_o, △), time constant of inactivation (τ_h, ●) and total open time during burst ($\tau_{open/burst}$, ○) as function of test potential. Data averaged from all experiments and plotted on semilogarithmic scale to aid in comparison.

potential, decreasing from 19 ms at −70 mV to 0·5 ms at −40 mV. The fast exponential component, τ_{l2}, which was not well resolved, shows no clear trend with depolarization.

The average slow time constant of the first latency distribution from all experiments is plotted in Fig. 7*B* as a function of test potential on a semilogarithmic scale. This time constant shows an approximately exponential dependence on membrane potential, decreasing e-fold for a 10 mV depolarization.

To what extent is τ_h a function of latency to opening? Figure 8*A* superimposes calculated first latency functions for a single channel on the observed ensemble-

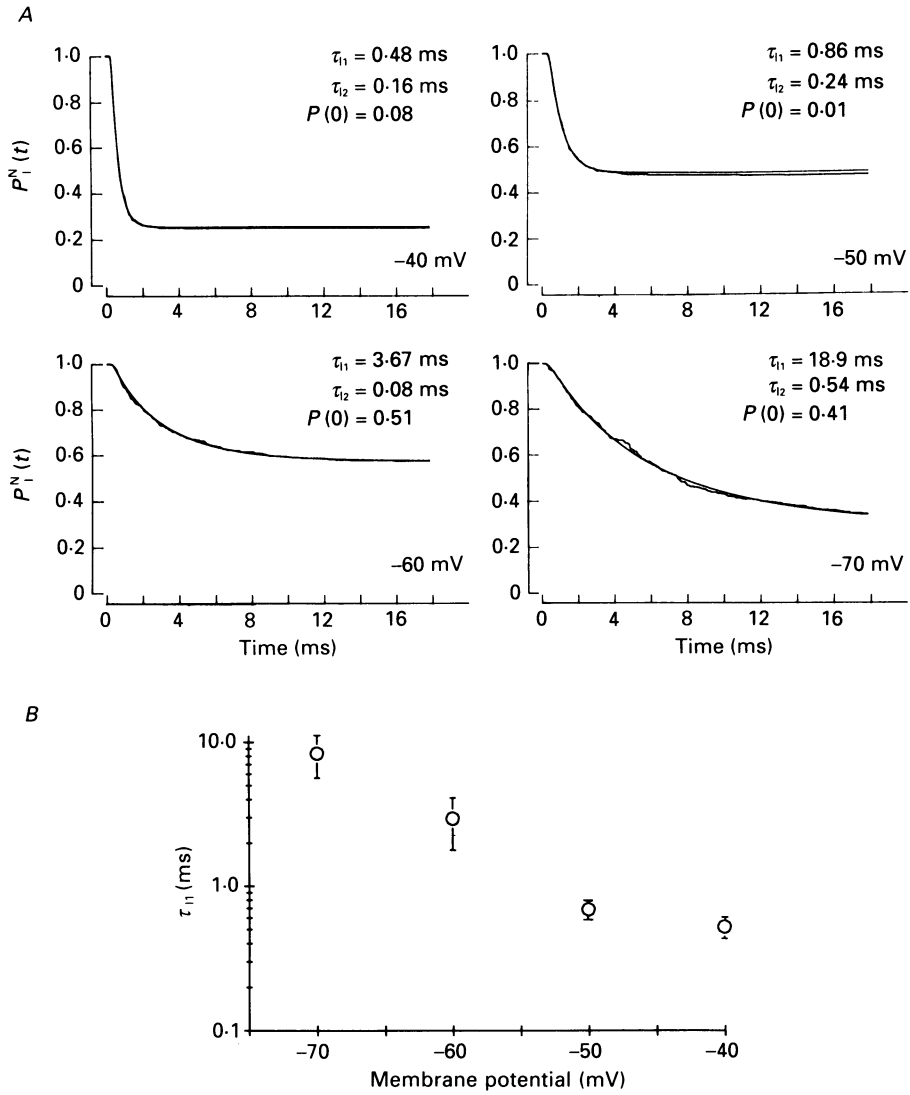

Fig. 7. First latency function for channel opening. *A*, cumulative histograms showing probability ($P_1^N(t)$) that a channel opening first occurs later than time t. Noisy traces show raw experimental data from six channel patches at different test potentials; smooth trace is fitted curve (eqn (3)). The values of the fast and slow exponential components (τ_{l1} and τ_{l2}) as well as probability that a resting channel does not open during pulse ($P(0)$) are indicated on each graph. Values are derived using eqns (2) and (3) in the Methods section and describe the behaviour of a single channel. Experimental conditions as in Fig. 2. *B*, dependence of slow first latency time constant on membrane potential. Data are averages from three to eight experiments and plotted on a semilogarithmic scale.

averaged current obtained from the same patch for a depolarization to the same test potential. The amplitude of the ensemble-averaged current has been scaled arbitrarily to allow for comparison. For depolarizations to −70 and −60 mV (near the foot of the activation curve), the time course of activation is indeed slow relative

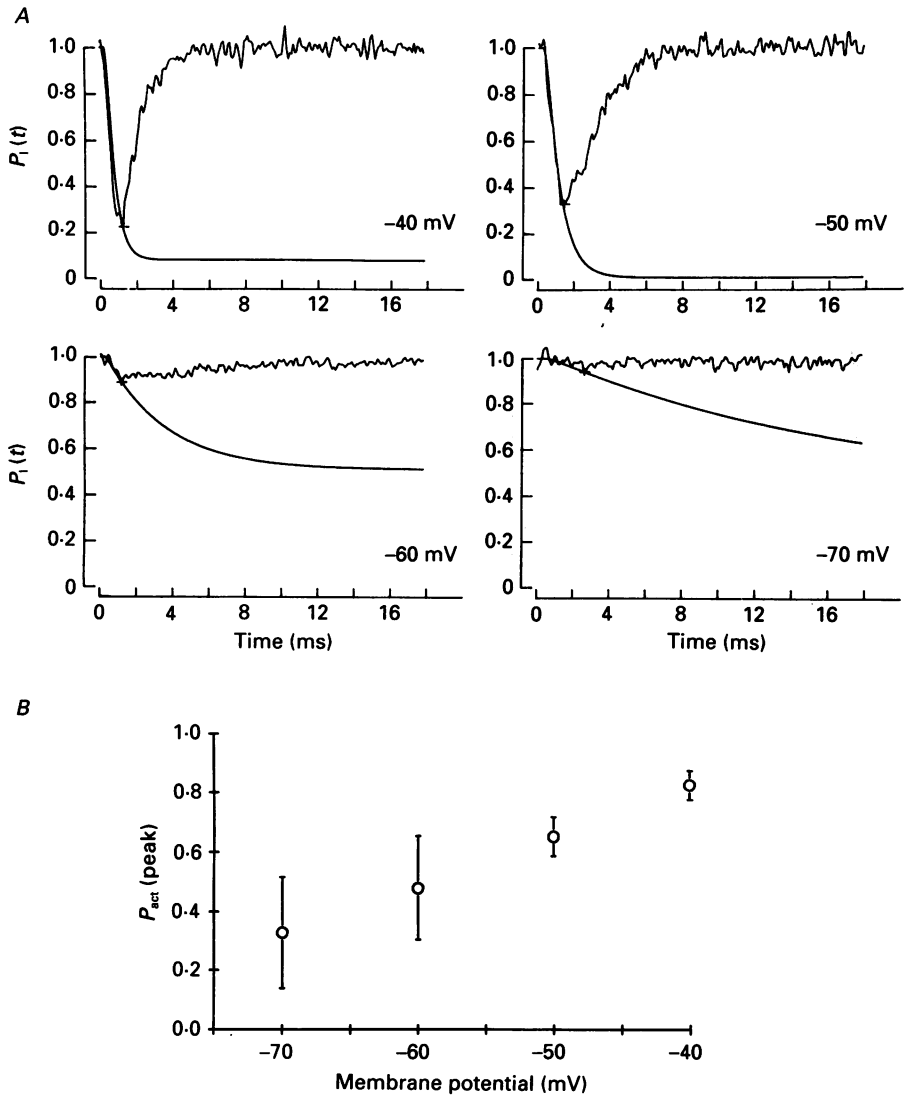

Fig. 8. *A*, comparison of first latency and ensemble-averaged sodium current. Smooth curve shows derived first latency function (eqn (2)) for single channel obtained from Fig. 7*A*. Noisy trace shows arbitrarily scaled, superimposed ensemble-averaged sodium current from same data used to obtain first latency. *B*, dependence of P_{act} (peak) on test potential. Data are averaged from all experiments.

to the ensemble-averaged sodium current. At the time of the peak inward current, only a small fraction of channels have opened and activation overlaps significantly with the apparent phase of 'inactivation' of the averaged current. Thus at these voltages, the apparent time course of inactivation depends to a significant extent on the time course of channel activation. However, with steps to −40 mV, the activation process is relatively fast. Now, by the time of the peak inward current, activation is nearly complete and there is relatively little overlap with the decay

phase of the averaged sodium current. Thus at the more depolarized test voltages, the first latency function should contribute little to the apparent rate of inactivation of the ensemble-averaged current.

The relationship between test potential and the completeness of channel activation at the time of peak inward current is summarized in Fig. 8*B*. Here P_{act}(peak) is defined as the fraction of channels that have activated by the time of peak inward sodium current, $(1-P_1(\text{peak}))$, normalized by the fraction of channels that eventually open, $(1-P(0))$. Thus, P_{act}(peak) is a measure of the probability that a channel has opened by the time of the peak ensemble-averaged current given that it opens at all during a depolarization. There is a clear trend for a greater fraction of channels to open by the time of the peak ensemble-averaged sodium current at more depolarized test potentials.

Sodium channel reopening

Although the activation process does not appear to play a major role in determining the apparent time course of inactivation of the ensemble-averaged sodium current at more depolarized test potentials, there is still a considerable discrepancy between single-channel open time, τ_o, and τ_h, even at -40 mV. One possibility is that a single channel opens more than once during a depolarization. In this case, τ_h should be related to the mean burst duration (τ_{burst}), the time from the first opening of a channel to the last closing of the same channel during a depolarization.

In most of our experiments, it was not possible to measure τ_{burst} directly since our patches generally contained several channels. Instead we have measured the total mean open time per burst ($\tau_{open/burst}$), given by $\bar{j}_b\tau_o$, where τ_o is mean open time and $\bar{j}_b$ is the number of openings per burst. This number ($\bar{j}_b$) depends on the probability that an open channel reopens, R, rather than inactivates, according to:

$$\bar{j}_b = 1/(1-R). \tag{9}$$

We obtained estimates for R by measuring the observed mean total number of openings per sweep, $\bar{j}'$, and the observed fraction of sweeps with no openings $P(0)'$ (see Theory). Both $\bar{j}'$ and $P(0)'$ were then corrected to account for missed openings and closings (see Appendix) to yield $\bar{j}$ and $P(0)$. We then obtained estimates for the transition probability A, that a resting channel opens, from eqn (4) and derived the probability R from eqn (5) (see Theory section).

These probabilities are plotted as a function of test potential in Fig. 9. At -70 mV, about half the resting channels directly inactivate without opening ($A = 0{\cdot}5$). As the membrane is depolarized, A approaches 1, i.e. nearly all resting channels enter the open state. At -70 mV, channels also show a substantial probability of reopening with $R = 0{\cdot}6$. At more positive potentials, R decreases so that at -40 mV, most open channels will inactivate, as opposed to returning to rest. The experimental values for $\bar{j}'$ and $P(0)'$ as well as the calculated values for $\bar{j}_b$, the number of openings per burst, are listed in Table 1. For steps to -60 and -70 mV, there are around two openings per burst on average. With a step to -40 mV, the mean number of openings per burst is only 1·1. These results confirm the qualitative impressions from Fig. 2; at negative test potentials a single channel can open several times before inactivating.

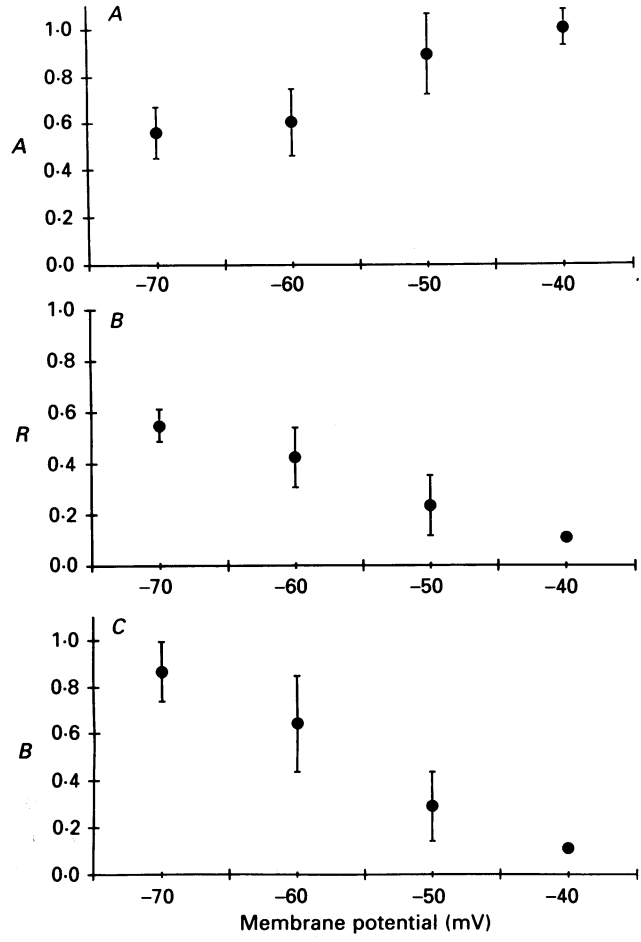

Fig. 9. Average Markov probabilities for channel transitions. *A*, dependence of *A*, probability that a resting channel opens, on test potential. *B*, dependence of *R*, probability that an open channel reopens, on test potential. *C*, dependence of *B*, probability that open channel returns to rest, on membrane potential.

However, at more positive test potentials, channels tend to open only once before inactivating, similar to the results of Aldrich *et al.* (1983).

Total open time during a burst, calculated from $\bar{j}_b$ and τ_o, is compared to measurements of τ_h in Fig. 6*B*. At -40 and -50 mV there is rather good agreement between $\tau_{open/burst}$ and τ_h, while at the negative potentials $\tau_{open/burst}$ is still substantially less than τ_h, reflecting the contribution of slow activation at these potentials.

Measurements of $\tau_{open/burst}$ provide a lower limit on burst duration since they neglect the contribution of closed time to burst duration. In one experiment with a patch containing a single channel, we were able to measure directly τ_{burst}. Figure 10 compares τ_o, $\tau_{open/burst}$, τ_{burst} and τ_h as a function of test potential from this experiment. These results show that there is relatively good agreement between τ_{burst} and τ_h over the entire range of test potentials. However, at the more negative test

voltages there is still a discrepancy between τ_{burst} and τ_h, reflecting the contribution of slow activation to τ_h near the threshold for channel activation.

Voltage dependence of channel closing

One major question regarding sodium channel kinetics is the degree to which inactivation from the open state is voltage dependent. Using the simplified model of Aldrich *et al.* (1983) (see (M1), Theory section), we have estimated rates for open channel inactivation (b) and closing (a) as well as the probability, B, that an open channel closes to the resting state. Figure 9*C* plots the relation between B and membrane potential. At -70 mV, B is close to 1 so that an open channel almost always closes to the resting state as opposed to inactivating. As the membrane is depolarized, B decreases so that at -40 mV, the vast number of transitions are from the open state to the inactivated state.

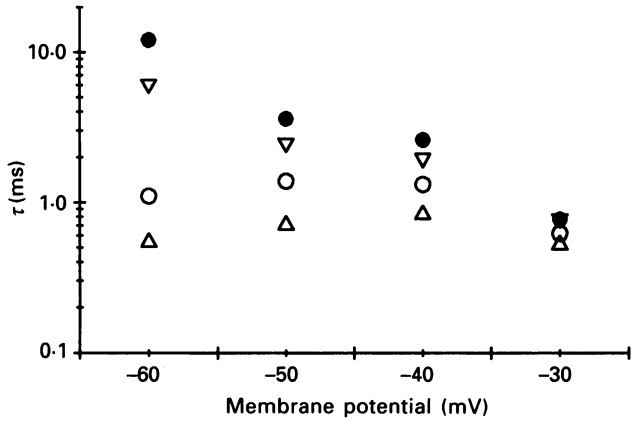

Fig. 10. Channel open time (τ_o, △), ensemble-averaged time constant of inactivation (τ_h, ●), total open time during burst ($\tau_{open/burst}$, ○) and burst duration (τ_{burst}, ▽) as function of test potential from one patch with only a single channel.

Using the measured values of τ_o and B, we have determined the individual rate constants a and b. Figure 11 plots their dependence on membrane potential. As seen here, both rates are apparently voltage dependent. The closing rate a shows an e-fold decrease for every 11 mV of depolarization while the inactivation rate b shows an e-fold increase for a 30 mV depolarization. This corresponds to an effective valency of around 2·2 charges for the process of closing to the resting state and 0·8 charges for the inactivation process. These results do not appear to be an artifact of analysis with multichannel patches since similar results were obtained with the single-channel patch. Here a showed an e-fold decrease for a 20 mV depolarization while b increased e-fold with a 22 mV depolarization.

Estimates for rates of open channel inactivation are limited by the fact that the Aldrich, Corey and Stevens analysis does not yield meaningful results over the entire voltage range for all experiments. For the most negative test potential of -70 mV, the analysis gave a probability B that is greater than one and negative rate constants for b in three out of six experiments. Only those experiments yielding positive values

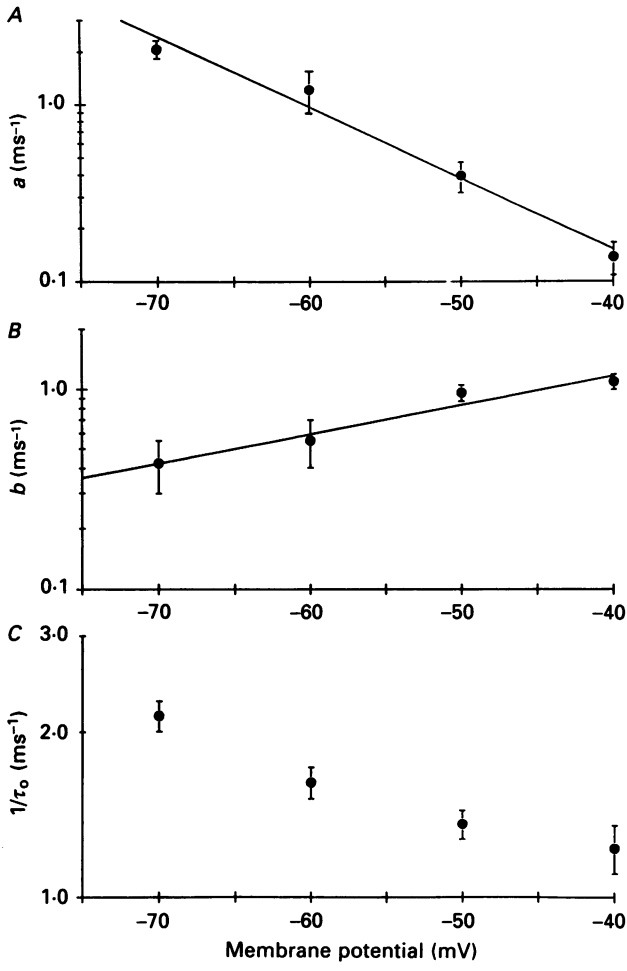

Fig. 11. Average kinetic constants for rate of open channel closing (a), rate of open channel inactivation (b) and 1/open time ($1/\tau_o$). Straight lines show calculated best fits to data using linear regression. A, closing rate of open channel decreases e-fold for 11 mV depolarization. B, rate of open channel inactivation increases e-fold for 30 mV depolarization. C, dependence of 1/open time on test potential.

for b are included in the plots of b and a (Fig. 11) and B (Fig. 9). Possible reasons for these problems are presented in the Discussion.

DISCUSSION

In this study, we have focused on the relative roles that sodium channel activation and inactivation play in determining the time course of decay of the macroscopic cardiac sodium current (i.e. the apparent rate of 'inactivation'). Our results show that the macroscopic kinetics depend on both channel activation and inactivation. Thus, with steps to negative potentials, where the opening of closed sodium channels is relatively slow, the kinetics of sodium current decay are dominated by the process

of activation. However, with steps to more positive voltages, where activation is quite rapid, the time course of sodium current decay largely reflects the process of channel inactivation. Thus the answer as to which reaction controls the overall time course of sodium current 'inactivation' depends on the voltage used to elicit sodium current, reflecting the underlying voltage dependence of sodium channel activation and inactivation.

Ensemble-averaged currents

To what extent are the rates of activation and inactivation voltage dependent? Since the initial studies of Hodgkin and Huxley, there has been general agreement that sodium channel activation is a steeply voltage-dependent process. However, the question of the voltage dependence of channel inactivation is more controversial. What is clear is that the time constant (or time constants) of decay of whole-cell sodium currents show a marked dependence on membrane potential, in both neuronal and cardiac cells. In the heart, the macroscopic time course of inactivation has been reported to consist of one (Ebihara & Johnson, 1980) or two exponential components, although the majority of the current relaxation is related to the fast component (Kunze *et al.* 1985; Patlak & Ortiz, 1985; Nilius, Benndorf & Markwardt, 1986; Follmer, Ten Eick & Yeh, 1987; Fozzard, Hanck, Makielski, Scanley & Sheets 1987; Yatani, Kirsch, Possani & Brown, 1988). In this study, we have approximated the time course of decay of the ensemble-averaged sodium channel currents from cell-attached patch recordings with a single exponential function. In agreement with previous results (Grant & Starmer, 1987; Makielski, Sheets, Hanck, January & Fozzard, 1987), we find that the time constant of current decay (τ_h) shows a marked dependence on membrane potential, decreasing e-fold for a 15 mV depolarization.

Another indication of the voltage dependence of channel inactivation is the marked dependence of steady-state inactivation on holding potential (Fig. 4*A*). As in other single-channel studies (Cachelin *et al.* 1983; Kunze *et al.* 1985; Grant & Starmer, 1987), we find that the voltage dependence of steady-state inactivation is shifted by 20–30 mV in the hyperpolarizing direction compared to the normal mid-point of inactivation in canine ventricular myocytes (Tseng, Robinson & Hoffman, 1987). The mechanism for this shift, which is seen in both cell-free and cell-attached patches, is not known, although we find that in cell-attached recordings, where the bath contains normal Tyrode solution, the shift is generally absent. There appears to be much less of a shift in the activation process, as judged by the relatively normal threshold for sodium current activation (around −70 mV). Despite the shift in position of the inactivation curve, its steepness (characterized by the slope factor k) is very similar to that seen with conventional voltage clamp techniques where little or no shift is present (e.g. Colatsky, 1980). However, the steepness is significantly less than the 2–3 mV slope factor of Tseng *et al.* (1987) obtained from measurements of $\dot{V}_{max}$ in the same preparations of canine ventricular cells used in these studies.

Single-channel analysis

Although the above results suggest (as they did to Hodgkin and Huxley) a genuine voltage-dependent inactivation process, several independent lines of evidence suggest that inactivation (at least from the open state) is voltage independent and only

appears voltage dependent because it is kinetically coupled to the voltage-dependent activation process (Armstrong & Bezanilla, 1977; Bezanilla & Armstrong, 1977; Aldrich *et al.* 1983). On the other hand, Vandenberg & Horn (1984) have presented evidence for voltage-dependent inactivation from GH3 cells based on single-channel recordings. Grant & Starmer (1987) have also suggested that inactivation of rabbit cardiac sodium channels may be voltage dependent based on a comparison of normal and batrachotoxin-modified sodium channel kinetics. Using an approach similar to that used by Aldrich *et al.* (1983), we find that the rate of inactivation from the open state shows a modest voltage dependence, corresponding to a valency of 0·8 charges. This is roughly one-third the apparent voltage dependence of the activation reaction (2·2 charges) and accounts for roughly one-half of the voltage dependence of the rate of inactivation of the ensemble-averaged sodium current.

As the Aldrich, Corey and Stevens (Aldrich *et al.* 1983) three-state model (M1) is clearly a simplified scheme, the question arises as to how much confidence we can attach to our conclusions based on this analysis. Because of this uncertainty, we have divided our conclusions below into model-independent and model-dependent categories.

Model-independent conclusions

How fast is channel opening compared to the macroscopic sodium current kinetics? Here we were able to determine directly the rate of channel opening from the first latency function and compare it to the ensemble-averaged current. The first latency function could be fitted reasonably well with two exponential components, suggesting two closed states, although the faster exponential component was not well resolved. By measuring the fraction of channels that open by the peak of the ensemble-averaged current, we found that with steps to -40 mV, most channels open by the time of peak inward current. This result is in agreement with the Hodgkin–Huxley model as well as voltage clamp results in squid giant axon (Armstrong & Bezanilla, 1977) and frog muscle (Gonoi & Hille, 1987). However, with steps to more negative potentials, especially near the threshold for channel activation, a significant fraction of sodium channels do not open by the time of peak inward current, in agreement with the findings of Aldrich *et al.* (1983). Thus at these negative potentials, the time course of the macroscopic current decay is largely determined by the time course of channel opening. The fact that the fraction of channels that opens by the peak of the ensemble-averaged current increases with more positive depolarizing test pulses suggests that the voltage dependence of the overall rate of activation is greater than the voltage dependence of the rate of open channel inactivation.

One major difference between our results and those of Aldrich *et al.* (1983) lies in the voltage dependence of channel open time. While Aldrich *et al.* found that mean open time was relatively independent of membrane potential, we find a significant increase in open time as the membrane is depolarized from -70 to -40 mV, in agreement with previous studies (Fenwick, Marty & Neher, 1982; Kunze *et al.* 1985; Grant & Starmer, 1987).

A second difference with the results of Aldrich *et al.* lies in estimates of the number of openings per sweep. At negative potentials, channels generally open several times

before inactivating, although at −40 mV channels tend to open only once. In contrast, Aldrich *et al.* found that over a wide range of potentials, channels only open a single time before inactivating. Our finding of multiple openings is not an artifact resulting from underestimating the number of channels in multichannel patches since in an experiment from a patch that contained a single channel, similar results were obtained.

A consequence of multiple openings is that the macroscopic time course of inactivation reflects the open burst duration (time from first opening to last closing) and not the duration of a single opening. Interestingly, the Hodgkin–Huxley model predicts that a channel will open several times before inactivating. Since in the Hodgkin–Huxley model, the rates of open and closed channel inactivation are the same, the mean burst duration is equal to the reciprocal of the rate of inactivation.

The results obtained from the one patch with a single channel (see Table 1) also contribute qualitative information concerning the rates of channel transitions because of the biphasic relation between mean open time and test potential (also seen by Grant & Starmer, 1987). If we assume that the open channel shuts by either inactivating or returning to a closed state and that the rates of these reactions depend monotonically on voltage, the presence of a maximum in the open time *vs.* voltage relation implies that the two rates are voltage dependent in opposing directions. As the probability of reopening decreases with stronger depolarizations, the rate of inactivation must increase with depolarization and the rate of closing must decrease.

Model-dependent results

To determine explicitly the rate constants for individual gating steps requires either a specific model for sodium channel gating or a chemical modification of the channel to isolate kinetic processes. Although the Aldrich, Corey and Stevens three-state model (M1) is an oversimplification of sodium channel kinetics since it contains only a single resting closed state, a number of more realistic and complicated models can be formally reduced to the model of Aldrich *et al.* (1983) (M1) for the purpose of extracting rates of open channel inactivation (b) and closing to a resting state (a). Thus, all models where inactivation occurs from either the open state or a single closed resting state that immediately precedes channel opening and where the inactive state is absorbing are compatible with the approach of Aldrich *et al.* For example, a linear activation scheme of the following form:

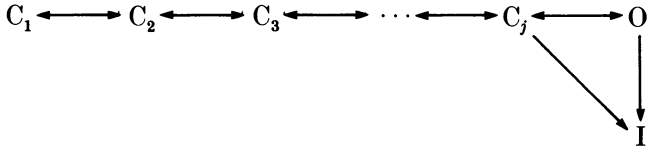

(M2)

allows for multiple exponential components in the first latency distribution and is consistent with the above criteria. In fact, Horn & Vandenberg (1984) found that this general type of model provided a good fit to their data for sodium channel kinetics in GH3 cells.

However, several groups have reported that the approach of Aldrich *et al.* is

inadequate, yielding negative rate constants and probabilities greater than one (Vandenberg & Horn, 1984; Kunze *et al.* 1985; Grant & Starmer, 1987). The failure of the approach could result from an inadequacy of the models (M1) and (M2) in describing sodium channel kinetics (i.e. significant inactivation from multiple closed states), a non-absorbing inactivated state or experimental errors in determining various parameters. Vandenberg & Horn (1984) concluded that the negative rate constants resulted from a small but finite probability that an inactivated channel can reopen, violating the assumption of an absorbing inactive state. Kunze *et al.* (1985) suggested that the failure of the approach for rat cardiac sodium channels was due to the inadequacy of the basic model (M1) and proposed a more complex kinetic scheme. In all cases, the failure of the model appears to result from the number of observed openings being in excess of the maximal number permitted from independent estimates of A, the probability that a resting channel opens.

Like Kunze *et al.* (1985), we found that the rates derived explicitly using the model (M2) were quite dependent on estimates of the number of channels in a patch and the value for resting availability (h_∞). However, by using stable patches where N was constant, by determining h_∞ before and after a run, and by using a relatively depolarized holding potential to provide an adequate number of nulls to estimate the probability A, we generally obtained non-negative estimates for a and b. With steps to -40 and -50 mV, the method of Aldrich *et al.* yielded realizable (i.e. non-negative) results in all cases. With steps to -60 mV, realizable rates were determined in four of five experiments. With steps to -70 mV, realizable rates were determined in three out of six experiments. In all cases, failure of the model was expressed in terms of values for the probability B, that an open channel closes to a resting state, being greater than 1 and negative values for b, the rate of open channel inactivation.

As mentioned above, a likely reason for the failure of the model is a small probability for channel reopening from the inactivated state at these negative test potentials. In fact, a similar trend can be seen in the results of Kunze *et al.* (1985), where the model of Aldrich *et al.* yields valid results for parameters at more positive test potentials. If kinetic schemes of the type shown in models (M1) or (M2) were invalid, one might expect failures of the model at the more positive potentials as well.

A second possible reason for the failure of the model is that when B is close to 1, at negative potentials, small errors in estimating the number of openings per sweep can lead to estimates for B that exceed 1. These errors could be due to false openings resulting from baseline noise that exceeds the threshold for channel detection or statistical variation in estimating the mean number of openings per sweep, $\bar{j}$, from a finite number of sweeps. Thus, for the model (M1) the expected variance in $\bar{j}$ estimated from a single sweep is given by:

$$\mathrm{var}(\bar{j}) = \frac{A(1-A+AB)}{(1-AB)^2}. \tag{10}$$

For an experiment with a total of T sweeps, the variance is given by $\mathrm{var}(\bar{j})/T$. Thus, in an experiment with 150 sweeps, where the true values for $A = 0{\cdot}5$ and for $B = 0{\cdot}9$, the expected value for $\bar{j}$ is $0{\cdot}91 \pm 0{\cdot}1$. If a particular experiment yielded a value for $\bar{j}$ that was one standard deviation larger than the expected mean, the derived estimate for B would be greater than 1.

As the Aldrich *et al.* analysis yields consistent, well-behaved results at more positive voltages, we feel that it provides a reasonable approximation to the behaviour of canine cardiac sodium channels for the purpose of estimating rates of open-channel inactivation and closing to a resting state. Our results suggest that the probability of open-channel inactivation is voltage dependent, with B decreasing from 0·8 to 0·1 as the magnitude of the depolarization increases. The rate of open-channel inactivation, b, increases e-fold for a 30 mV depolarization, while the rate of closing to a resting state, a, shows an e-fold decrease for an 11 mV depolarization. Aldrich & Stevens (1987) in their most extensive study found that the closing rate a decreased e-fold for every 7·0 mV (calculated from their data), but inactivation had little voltage dependence, with b increasing e-fold for a 52·2 mV depolarization. Vandenberg & Horn (1984), using the method of maximum likelihood, obtained voltage dependencies for the rates a and b that corresponded to an e-fold decrease per 18·7 mV depolarization and an e-fold increase per 12·7 mV depolarization, respectively.

Other investigators have used chemical modification to estimate the transition rates. Horn, Vandenberg & Lange (1984) have compared control and NBA-treated patches. Although probability of open-channel inactivation increased from 0·39 to 0·94 with depolarization, the calculated inactivation rate increased only e-fold per 34 mV. Grant & Starmer (1987) found qualitatively similar results using batrachotoxin; the rate of single-channel inactivation increased with depolarization while the rate of closing to a resting state decreased.

The rather wide discrepancies in estimates for channel inactivation could reflect heterogeneity in sodium channel structure from different tissues. Three different sodium channel cDNA clones have been isolated from rat brain (Noda, Ikeda, Kayano, Suzuki, Takeshima, Kurasaki, Takahashi & Numa, 1986). From pharmacological measurements, cardiac sodium channels are likely to represent a structurally distinct class of proteins. It is interesting to speculate that sodium channel types may have evolved slight differences in structure to support different physiological roles. Thus in axons and cardiac cells, where rapid conduction is important, sodium channels show rapid activation relative to inactivation. As a result, most channels will open during a brief depolarization, such as a conducted action potential, and provide for a large inward current. In neuronal cell bodies and exocrine gland cells, it may be more desirable to have channels that are less efficient, generating a more slowly rising action potential with a higher threshold that would be better suited for integrating several different synaptic inputs before firing a spike. By studying single sodium channel currents expressed from cDNA clones in a system such as the *Xenopus* oocyte, such questions may soon be resolved.

APPENDIX

Correcting for missed openings and missed closings

Missed short openings and short closings, due to the limited bandwidth of the recordings, can introduce several errors in the analysis. Colquhoun & Sigworth (1983) have presented an approach to correct for both types of missed events simultaneously, in the simple case of a single closed and single open state. Here we

extend this to include an inactivation state as in the Aldrich, Corey & Stevens model (M1).

According to this approach, we will observe a series of i openings and $i-1$ closings as a single extended opening if the first open duration is greater than our threshold for detection, Q, and all $i-1$ closings are shorter than Q. With the 50% threshold for event detection, $Q = 0{\cdot}179/f_c$ s where f_c is the cut-off frequency. If n is the mean number of openings per extended opening, t_o' is given by:

$$t_o' = t_o + Q + (n-1)(t_o + t_{cm}), \tag{A 1}$$

where t_{cm}, the mean duration of the undetected (missed) closing, is given by:

$$t_{cm} = 1/t_c \int_0^Q t \exp(-t/t_c)\, dt = \frac{t_c - (t_c + Q)D}{1-D}, \tag{A 2}$$

where t_c is the true mean closed time between openings and D is the probability of a closing lasting longer than Q, given by $\exp(-Q/t_c)$.

The next step is to evaluate n, the mean number of openings per extended opening. There are two ways an extended opening can be terminated. First, the open channel can close to state C, remain there for a time greater than Q and reopen. The probability of observing a long closure is given by D. Second, the channel can inactivate, either directly from O or after first returning to C. This probability is just the probability that an open channel does not reopen, given by $1-R$ (or $[1-AB]$ according to the model of Aldrich *et al.* (1983)).

Thus the probability of observing one opening per extended opening is given by:

$$P(1) = \text{probability[inactivate] or probability[reopen and long closure]}$$

or

$$P(1) = (1-R) + RD = [1-R(1-D)]. \tag{A 3}$$

The probability of two openings per extended opening is given by:

$$P(2) = \text{probability(reopens and short closure)}\ P(1)$$

or

$$P(2) = [R(1-D)][1-R(1-D)]. \tag{A 4}$$

In general,

$$P(i) = [R(1-D)]^{i-1}[1-R(1-D)]. \tag{A 5}$$

Thus the mean number of openings per extended opening (n) is given by:

$$n = \sum_{i=1}^{\infty} i[1-R(1-D)][R(1-D)]^{i-1} \tag{A 6}$$

or

$$n = \frac{1}{1-R(1-D)}. \tag{A 7}$$

Substituting eqns (A2) and (A7) into eqn (A1) yields:

$$t_o' = \frac{t_o + [t_c - D(t_c + Q)]/(1-D)}{1 - R(1-D)} + Q\frac{t_c - D(t_c + Q)}{(1-C)}. \quad \text{(A 8)}$$

Similarly we can derive an expression for t_c', the length of an apparent extended closed interval:

$$t_c' = \frac{t_c + [t_o - E(t_o + Q)]/(1-E)}{1 - R(1-E)} + Q\frac{t_o - E(t_o + Q)}{(1-E)}. \quad \text{(A 9)}$$

where E, the probability that an opening is greater than Q, is given by $\exp(-Q/t_o)$.

As t_o' and t_c' are what we determine experimentally, we wish to solve for t_o and t_c, the true open and closed times. Thus rearranging eqns (A8) and (A9) yields:

$$t_c = t_c'[1 - R(1-E)] - Q(1-R) - t_o R(1-E), \quad \text{(A 10)}$$

$$t_o = t_o'[1 - R(1-D)] - Q(1-R) - t_c R(1-D). \quad \text{(A 11)}$$

When $R = 1$, these expressions reduce to those of Colquhoun & Sigworth (1983).

In order to obtain corrected open and closed times, it is necessary to obtain an estimate for R, the probability that a channel reopens. According to the methods of Kunze *et al.* (1985) (see Theory section), R, can be obtained from measurements of the mean number of channel openings during a depolarization ($\bar{j}$). For a patch containing N channels with a given level of resting inactivation $(1 - h_\infty)$:

$$\bar{j} = \frac{N h_\infty A}{1 - R}. \quad \text{(A 12)}$$

A is the probability that a resting channel opens and can be determined from the fraction of sweeps with no openings according to:

$$P(0) = (1 - h_\infty A)^N. \quad \text{(A 13)}$$

The above expressions, however, need to be corrected for missed openings and closings. The observed probability of a null sweep, $P(0)'$, will overestimate the true probability $P(0)$ because of missed openings. Missed openings and missed closings will both contribute to an underestimate of $\bar{j}$. Kunze *et al.* (1985) have provided equations to correct both $\bar{j}'$ and $P(0)'$ for missed openings (but not missed closings). Thus, if $\bar{j}'$ and $P(0)'$ are the observed values:

$$\bar{j} = \bar{j}' \exp(Q/t_o), \quad \text{(A 14)}$$

and

$$P(0) = \frac{P(0)'(1 - RE) - E(1-R)}{1 - E}. \quad \text{(A 15)}$$

It is also possible to correct for missed closings as follows. Since n is the mean number of true openings per extended opening (due to missed closings) the true number of openings within all detected extended openings per sweep will be given by the product $n\bar{j}'$. However, there will also be some openings that are missed because they are too brief to be detected and are not part of an extended opening (i.e. they

follow a long closure). The number of such missed events is given by $\bar{j}[\exp(Q/t_o)-1]$. Thus, the true total number of openings per sweep, $\bar{j}$, will be given by:

$$\bar{j} = n\bar{j}' + \bar{j}'[\exp(Q/t_o)-1]. \quad \text{(A 16)}$$

We used a recursive computer program to solve for t_o,t_c, A and R given observed values for t_o',t_c', $P(0)'$ and $\bar{j}'$. In practice, the corrections for missed closings were small, less than 10%, although the correction for missed openings could be significant, especially at negative voltages where $t_o < 0{\cdot}5$ ms. Missed closings were less of a problem because at positive voltages where the closed time was brief, the probability of reopening (R) was small so that there were few closings followed by openings. At negative potentials, when R was larger, the mean closed time was also larger so that the probability of missing a closing was relatively low.

Note added in proof. Results similar to those presented here regarding the voltage dependence of open channel inactivation were reported for cardiac sodium channels in guinea-pig ventricular myocytes by Yue, Lawrence & Marban (1989).

We thank Dr Solomon Erulkar, Dr Lisa Ebihara and Ji-Fang Zhang for commenting on the manuscript, Kathrin Hilten and Bob Wooley for help in preparing the figures and Pat McLaughlin for preparing the cells. This work was supported by a program project grant HL-30557 from the NIH.

REFERENCES

ALDRICH, R. W., COREY, D. P. & STEVENS, C. F. (1983). A reinterpretation of mammalian sodium channel gating based on single channel recording. *Nature* **306**, 436–441.

ALDRICH, R. W. & STEVENS, C. F. (1987). Voltage-dependent gating of single sodium channels from mammalian neuroblastoma cells. *Journal of Neuroscience* **7**, 418–431.

ARMSTRONG, C. M. & BEZANILLA, F. (1977). Inactivation of the sodium channel. II. Gating current experiments. *Journal of General Physiology* **70**, 567–590.

BEZANILLA, F. & ARMSTRONG, C. M. (1977). Inactivation of the sodium channel. I. Sodium current experiments. *Journal of General Physiology* **70**, 549–566.

CACHELIN, A. B., DE PEYER, J. E., KOKUBUN, S. & REUTER, H. (1983). Sodium channels in cultured cardiac cells. *Journal of Physiology* **340**, 389–401.

COLATSKY, T. J. (1980). Voltage clamp measurements of sodium channel properties in rabbit cardiac Purkinje fibres. *Journal of Physiology* **305**, 215–234.

COLQUHOUN, D. & SIGWORTH, F. J. (1983). Fitting and statistical analysis of single-channel records. In *Single-Channel Recording*, ed. SAKMANN, B. & NEHER, E., pp. 191–263. New York and London: Plenum Press.

EBIHARA, L. & JOHNSON, E. A. (1980). Fast sodium current in cardiac muscle. A quantitative description. *Biophysics Journal* **32**, 779–790.

FENWICK, E. M., MARTY, A. & NEHER, E. (1982). Sodium and calcium channels in bovine chromaffin cells. *Journal of Physiology* **331**, 599–635.

FOLLMER, C. H., TEN EICK, R. E. & YEH, J. Z. (1987). Sodium current kinetics in cat atrial myocytes. *Journal of Physiology* **384**, 169–197.

FOZZARD, H. A., HANCK, D. A., MAKIELSKI, J. C., SCANLEY, B. E. & SHEETS, M. F. (1987). Sodium channels in cardiac Purkinje cells. *Experientia* **43**, 1162–1168.

FOZZARD, H. A., JANUARY, C. T. & MAKIELSKI, J. C. (1985). New studies of the excitatory sodium currents in heart muscle. *Circulation Research* **56**, 475–485.

GONOI, T. & HILLE, B. (1987). Gating of Na channels. Inactivation modifiers discriminate among models. *Journal of General Physiology* **89**, 253–274.

GRANT, A. O. & STARMER, C. F. (1987). Mechanisms of closure of cardiac sodium channels in rabbit ventricular myocytes: single-channel analysis. *Circulation Research* **60**, 897–913.

GRANT, A. O., STARMER, C. F. & STRAUSS, H. C. (1983). Unitary sodium channels in isolated cardiac myocytes of rabbit. *Circulation Research* **53**, 823–829.

HAMILL, O. P., MARTY, A., NEHER, E., SAKMANN, B. & SIGWORTH, F. J. (1981). Improved patch-clamp techniques for high-resolution current recording from cells and cell-free membrane patches. *Pflügers Archiv* **391**, 85–100.

HEWETT, K., LEGATO, M. J., DANILO JR, P. & ROBINSON, R. B. (1983). Isolated myocytes from adult canine left ventricle: Ca^{2+} tolerance, electrophysiology, and ultrastructure. *American Journal of Physiology* **245**, H830–839.

HODGKIN, A. L. & HUXLEY, A. F. (1952). A quantitative description of membrane current and its application to conduction and excitation in nerve. *Journal of Physiology* **117**, 500–544.

HORN, R. & VANDENBERG, C. A. (1984). Statistical properties of single sodium channels. *Journal of General Physiology* **84**, 505–534.

HORN, R., VANDENBERG, C. A. & LANGE, K. (1984). Statistical analysis of single sodium channels. Effects of *N*-bromoacetamide. *Biophysics Journal* **45**, 323–335.

KUNZE, D. L., LACERDA, A. E., WILSON, D. L. & BROWN, A. M. (1985). Cardiac Na currents and the inactivating, reopening, and waiting properties of single cardiac Na channels. *Journal of General Physiology* **86**, 691–719.

MAKIELSKI, J. C., SHEETS, M. F., HANCK, D. A., JANUARY, C. T. & FOZZARD, H. A. (1987). Sodium current in voltage clamped internally perfused canine cardiac Purkinje cells. *Biophysics Journal* **52**, 1–11.

NILIUS, B., BENNDORF, K. & MARKWARDT, F. (1986). Modified gating behaviour of aconitine treated single sodium channels from adult cardiac myocytes. *Pflügers Archiv* **407**, 691–693.

NODA, M., IKEDA, T., KAYANO, T., SUZUKI, H., TAKESHIMA, H., KURASAKI, M., TAKAHASHI, H. & NUMA, S. (1986). Existence of distinct sodium channel messenger RNAs in rat brain. *Nature* **320**, 188–192.

PATLAK, J. B. & ORTIZ, M. (1985). Slow currents through single sodium channels of the adult rat heart. *Journal of General Physiology* **86**, 89–104.

SIEGELBAUM, S. A., CAMARDO, S. A. & ROBINSON, R. B. (1986). Rapid activation of mammalian cardiac sodium channels. *Biophysics Journal* **49**, 53*a* (abstract).

TSENG, G. N., ROBINSON, R. B. & HOFFMAN, B. F. (1987). Passive properties and membrane currents of canine ventricular myocytes. *Journal of General Physiology* **90**, 671–701.

VANDENBERG, C. A. & HORN, R. (1984). Inactivation viewed through single sodium channels, *Journal of General Physiology* **84**, 535–564.

YATANI, A., KIRSCH, G. E., POSSANI, L. D. & BROWN, A. M. (1988). Effects of New World scorpion toxins on single-channel and whole cell cardiac sodium currents. *American Journal of Physiology* **254**, H443–451.

YUE, D. T., LAWRENCE, J. H. & MARBAN, M. (1989). Two molecular transitions influence cardiac sodium channel gating. *Science* (in the Press).